mathematics

MDPI

Article

Portfolio Selection with Hierarchical Isomorphic Risk Aversion

Wan-Yi Chiu

Department of Finance, National United University, Miaoli 360302, Taiwan; wychiu@nuu.edu.tw

Abstract: Researchers usually specify risk aversion coefficients from 1 (lowest) to M (highest) for a portfolio to indicate active or passive approaches. How effective is this practice? Recent studies suggest that the global minimum variance portfolio (GMVP) is statistically equivalent to portfolios with extensive risk aversion coefficients (the GMVP-equivalent). Expressing the risk aversion coefficient as a Taylor series of the target return and efficient set constants, we generalize the previous result to the non-GMVP-equivalents and segment mean-variance portfolios according to a hierarchy of risk aversion coefficients. In this paper, we show that hierarchical risk aversion coefficients are superior to isometric attributes.

Keywords: portfolio optimization; mean-variance; risk aversion coefficient; isomorphic hierarchy; isometric attribute

MSC: 62P05; 90C20

1. Introduction

Investors want clarity in their decisions associated with the risk–return tradeoff, which calls for precise risk tolerance given a target return. Variants of Markowitz [1] mean-variance analysis (MVA), such as the mean-variance utility (MVU), have been used to determine the relationship between an investor's risk tolerance and the risk–return tradeoff (see Stevens [2], Kan and Zhou [3]). In the MVU framework, the risk aversion coefficient γ measures the marginal reward an investor requires to take on more risk (in terms of variance) compared with the global minimum variance portfolio (GMVP, with an infinite γ). This measure provides insight into whether a portfolio assumes sufficient risk to achieve an expected return, where a lower γ indicates a higher target return and more significant portfolio risk. Although the investor's risk aversion coefficient appears stable on the time horizon, it may be substantially violated after a remarkable financial crisis. For instance, Jackwerth [4] indicated that the implied risk aversion functions using the option price and realized returns as indices changed shape dramatically around the 1987 crash. Guisoa et al. [5] have also indicated that the risk aversion of investors increased following the 2008 crisis.

Previous MVU studies have either employed estimated risk aversion coefficients or specified γ as an isometric coverage valued from 1 (the lowest risk aversion) to M (the highest risk aversion) for a portfolio, with these values reflecting active and passive portfolios, respectively. For instance, Bliss and Panigirtzoglou [6] have shown that the option-implied estimates of the S&P500 have horizon dependence values of 4.36 (the lowest), 5.22, 6.33, 8.44, 10.38, and 15.97 (the highest), for an average of $\gamma = 8.46$. Likewise, Bliss and Panigirtzoglou estimated that $\gamma = 0.93$ for the FTSE100 average, while the most conservative value was $\gamma = 1.52$. Alternatively, Stambaugh [7]directly used $\gamma = 1, 3$, and 5 to approximate an investor's relative risk aversion coefficients. Brandt and Santa-Clara [8] employed quadratic utility with $\gamma = 5$ to test asset pricing. DeMiguel et al. [9] employed $\gamma = 1, 2, 3, 4, 5$, and 10 to check the robustness of portfolio performance. Practitioners often utilize values of 1 (lowest risk aversion) to 5 (highest risk aversion) for γ. Overall, Aït-Sahalia and Lo [10] concluded based on various studies that the estimated constant relative

check for updates

Citation: Chiu, W.-Y. Portfolio Selection with Hierarchical Isomorphic Risk Aversion. *Mathematics* **2024**, *12*, 3375. https://doi.org/10.3390/math12213375

Academic Editor: Andrea Scozzari

Received: 10 September 2024
Revised: 25 October 2024
Accepted: 25 October 2024
Published: 28 October 2024

Copyright: © 2024 by the author. Licensee MDPI, Basel, Switzerland. This article is an open access article distributed under the terms and conditions of the Creative Commons Attribution (CC BY) license (https://creativecommons.org/licenses/by/4.0/).

risk aversion coefficients range between 0 and 60. Meanwhile, Bodnar and Okhrin [11] indicated that the typical γ values used in empirical applications range between 1 and 50.

An investor with low or moderate risk aversion may build a portfolio falling outside the GMVP equivalent. For example, Das et al. [12,13] illustrated a portfolio pyramid based on different levels of γ, in which the top, middle, and bottom of the pyramid are the mental accounts for bequest (with a low value of $\gamma = 0.8773$), education (with a moderate value of $\gamma = 2.7063$), and retirement (with a higher value of $\gamma = 3.7950$) goals, respectively. These goal-based portfolios have received considerable attention since the 2008–2009 crisis, when investors realized that chasing high returns could negatively impact long-term wealth accumulation. Notably, goal-based investing emphasizes attaining life goals, including saving for children's education, building a retirement nest egg, and leaving an inheritance, in addition to coping with large medical expenses in retirement. De Nardi et al. [14] and De Nardi and Yang [15] have indicated that leaving an inheritance is one of the major savings goals of U.S. households. Under the goal-based investing framework, the bequest portfolio (with a very low γ) satisfies all the scenarios of a high risk-taking ability portfolio: the time horizon is greater than 10 years, the individual has no significant liquidity needs for at least 10 years, and sufficient outside income and assets are available to maintain their standard of living (e.g., current income, access to credit, cash savings, and insurance) in case of an emergency. Meanwhile, asset allocation for an education fund (with a moderate γ) might have a sufficient time horizon for overweighting equities to achieve a higher target return. In contrast, asset allocation for a retirement portfolio (with a higher γ) focuses entirely on safe assets.

In practice, we trace the frontier using estimates of the mean and covariance matrix of returns. The finite sample distribution must be analyzed to determine what estimation risk affects the efficient set constants and sample frontier (see Dickinson [16], Klein and Bawa [17], Jobson and Korkie [18], Best and Grauer [19], Jobson [20], Britten-Jones [21], Okhrin and Schmid [22], Kan and Smith [23]). However, while much progress has been made in studying the sample frontier distribution, comparatively little progress has been made in investigating the statistical inference of γ. Several studies have attempted to determine the γ bound for the GMVP based on various test statistics; for instance, Bodnar and Okhrin [11] analyzed the role of risk aversion coefficients in portfolio choices under estimation risk, while Chiu [24] applied this methodology to the minimum variance futures hedge. These studies suggest that portfolios with extensive risk aversion coefficients are statistically equivalent to the GMVP. Hereafter, the terms GMVP-equivalents and μ_g-γ-equivalents refer to these portfolios unless otherwise stated; similarly, μ_{p_i}-γ-equivalents refer to portfolios that are statistically equivalent to the efficient portfolio with a target return $\mu_{p_i} \leq \mu_p < \mu_{p_{i+1}}$ based on the statistics of γ. Combining the sample frontier's upper confidence limit and the μ_p-γ-equivalent, we then build the μ_p-σ_p^2-γ-equivalent area for a target return μ_p. Nevertheless, these results are restricted to the GMVP strategy, and no general solution exists for other risk aversion coefficients.

In this study, we integrate the results of Bodnar and Okhrin [11] and the sample distributions of efficient set constants into an approximation approach to segment the mean-variance investment opportunities. Specifically, we focus on the statistical validation of non-GMVP-equivalent portfolios. Thus, we first establish the relationship between the risk aversion coefficient and the efficient set constants. The intuition is that an MVU portfolio is equivalent to the MVA strategy in the upper frontier section (see Bodnar et al. [11]). Equating the portfolio weights of both approaches, we first express the subjective risk aversion coefficient as a Taylor series of the ratio of the GMVP's return to the target return. Under the standard assumptions, which require the normally distributed returns and the riskless return to be smaller than the GMVP return of risky assets, we then analytically derive the sample moments based on the first- and second-degree Taylor polynomials of the estimated risk aversion coefficients.

Finally, we conduct an experiment using Dow Jones Industrial Average (DJIA) stocks. This experiment is composed of three parts: First, we construct the GMVP-equivalent

γ bound based on three test statistics (the portfolio variance's χ^2-statistic, the return's t-statistic, and the z-statistic). Then, we approximate the μ_p-γ-equivalent bounds for the higher target returns. We confine the estimates to the first- and second-degree Taylor polynomials in order to reduce the computational burden. Although the differences between the two assessments may be dramatic around the GMVP return, the conclusion holds for non-GMVP-equivalent cases. Finally, portfolios are simulated to examine the potential factors of the hierarchical tiers. We find that the γ attributes are clustered together in certain higher-γ cases and that the portfolio size is a critical determinant of the tiers. These findings show that the commonly used γ assignment may not be sufficiently clear to distinguish the risk attitudes of investors. Therefore, we suggest transferring the isometric attributes into an isomorphic hierarchy of risk aversion coefficients.

The rest of this paper proceeds as follows: in Section 2, the risk aversion coefficient is expressed as a Taylor series of the target return and efficient set constants; in Section 3, the approximation and the isomorphic hierarchy of risk aversion coefficients are developed; Section 4 illustrates the various bounds of the risk aversion coefficients and portfolio simulations to examine the hierarchical factors; finally, Section 5 presents the conclusions.

2. The Model

This section outlines several well known portfolio optimizers and their preliminary properties to address the estimation of risk aversion coefficients.

2.1. Mean-Variance Optimization

Assume that the investment universe Ω_N has a risky returns vector $r \in \mathbb{R}^N$ with expectation vector $\mu \in \mathbb{R}^N$ and positive definite covariance matrix $\Sigma \in \mathbb{R}^{N\times N}$. Additionally, denote the vector of ones as $\iota \in \mathbb{R}^N$. Markowitz's [1] mean-variance optimization minimizes the portfolio variance for a given target return (μ_p):

$$\text{(MVA)} \quad \min_{\omega_p} \omega_p'\Sigma\omega_p \quad \text{subject to } \omega_p'\mu = \mu_p \text{ and } \omega_p'\iota = 1. \tag{1}$$

Merton [25] and Jobson [20] defined the efficient set constants and their mappings as follows:

$$a = \mu'\Sigma^{-1}\mu, \quad b = \iota'\Sigma^{-1}\mu, \quad c = \iota'\Sigma^{-1}\iota, \quad \psi = \tfrac{ac-b^2}{c}, \quad \mu_g = \tfrac{b}{c}, \quad \sigma_g^2 = \tfrac{1}{c}. \tag{2}$$

With appropriate adjustments of the notation, Roll's [26] optimal portfolio weight, portfolio variance, and orthogonal portfolio return μ_z relative to μ_p are expressed as

$$\omega_p = \tfrac{(\mu_p-\mu_g)\Sigma^{-1}(\mu-r_z\iota)}{\psi}, \quad \sigma_p^2 = \sigma_g^2\left[1+\tfrac{\left((\mu_p-\mu_g)/\sigma_g\right)^2}{\psi}\right], \quad \mu_z = \tfrac{b\mu_p-a}{c\mu_p-b}. \tag{3}$$

Substituting different values for μ_p in the (σ_p^2, μ_p) plane, we can trace out the population minimum-variance frontier (denoted as EF_p) in the mean-variance space. The GMVP is located at (σ_g^2, μ_g).

2.2. Mean-Variance Utility Optimization

Although MVA investors logically build portfolios based on their risk–return tradeoff, they do not explicitly reveal their attitudes towards risk. As risk aversion is not an objectively measurable quantity, researchers often approximate the MVA with various forms of utility functions under certain conditions (see Kroll et al. [27] and Das et al. [12]). When the returns are multivariate normally distributed, we can maximize the expected returns that remove the risk penalty, which is measured as the product of the risk aversion coefficient and the variance of the return (see Ingersoll [28] and Okhrin and Schmid [22]):

$$\text{(MVU)} \quad \max_{\omega_\gamma}\left(\omega_\gamma'\mu - \frac{\gamma}{2}\omega_\gamma'\Sigma\omega_\gamma\right) \quad \text{subject to } \omega_\gamma'\iota = 1 \tag{4}$$

where γ is a positive risk aversion coefficient that measures the marginal reward an investor requires to take on more risk. The Lagrange method provides the optimal weights, return, and variance, expressed as follows:

$$\omega_\gamma = \frac{1}{\gamma}\left[\Sigma^{-1}\mu - \left(\frac{b-\gamma}{c}\right)\Sigma^{-1}\iota\right], \quad \mu_\gamma = \frac{\psi}{\gamma} + \mu_g, \quad \sigma_\gamma^2 = \frac{\psi}{\gamma^2} + \sigma_g^2. \tag{5}$$

Likewise, by substituting different values of γ into $(\sigma_\gamma^2, \mu_\gamma)$, we can trace out a positively-sloped frontier (denoted as EF_γ) in the mean-variance space. In this situation, a conservative MVU investor with a higher risk aversion coefficient will build a portfolio that is close to the GMVP; conversely, the portfolio choice moves away from the GMVP as γ declines.

2.3. Relationship Between MVU and MVA

To estimate the risk aversion coefficient, we need to link γ with the efficient set constants. Our first result presents an alternative characteristic of γ in the mean-variance plane.

Theorem 1. *Given a target return μ_p on the upper frontier boundary, the MVU portfolio has the following weight representation:*

$$\omega_\gamma = \frac{\Sigma^{-1}(\mu - r_*\iota)}{\gamma} \quad \textit{with } r_* = \frac{b-\gamma}{c}. \tag{6}$$

Under the standard condition $\mu_p > \mu_g > 0$, the positive risk aversion coefficient can be expressed as

$$\gamma = \frac{\psi}{\mu_p}\left[1 + \left(\frac{\mu_g}{\mu_p}\right) + \left(\frac{\mu_g}{\mu_p}\right)^2 + \cdots\right]. \tag{7}$$

Proof. Figure 1 plots the relation between the MVU risk aversion coefficient and the MVU frontier. Assume that the secant line through the GMVP and the MVU portfolio $(\sigma_\gamma^2, \mu_\gamma)$ has return intercept r_*. We make three observations. First, the frontier EF_γ always resides on the upper boundary of the traditional frontier EF_p, as

$$\frac{(\mu_\gamma - \mu_g)^2}{\psi} + \sigma_g^2 = \frac{\left(\frac{\psi}{\gamma} + \mu_g - \mu_g\right)^2}{\psi} + \sigma_g^2 = \frac{\psi}{\gamma^2} + \sigma_g^2 = \sigma_\gamma^2.$$

Second, the secant line through the frontier vertex and the MVU portfolio has the following slope:

$$\frac{\mu_\gamma - \mu_g}{\sigma_\gamma^2 - \sigma_g^2} = \gamma = \frac{\mu_\gamma - r_*}{\sigma_\gamma^2 - 0}.$$

Thus, we reduce the return intercept to $r_* = \frac{b-\gamma}{c}$ and rewrite the weight as

$$\omega_\gamma = \frac{1}{\gamma}\left[\Sigma^{-1}\mu - \left(\frac{b-\gamma}{c}\right)\Sigma^{-1}\iota\right] = \frac{\Sigma^{-1}(\mu - r_*\iota)}{\gamma}.$$

Finally, without loss of generality, we can assume that the riskless return is smaller than the GMVP return of risky assets. The sufficient condition follows from the positivity of γ when μ_p is greater than μ_g. Setting ω_γ equal to ω_p in Equation (3) leads to the following Taylor expansion:

$$\gamma = \frac{ac - b^2}{c\mu_p - b} = \frac{\psi}{\mu_p - \mu_g} = \frac{\psi}{\mu_p}\left[1 + \left(\frac{\mu_g}{\mu_p}\right) + \left(\frac{\mu_g}{\mu_p}\right)^2 + \cdots\right].$$

This completes the proof. □

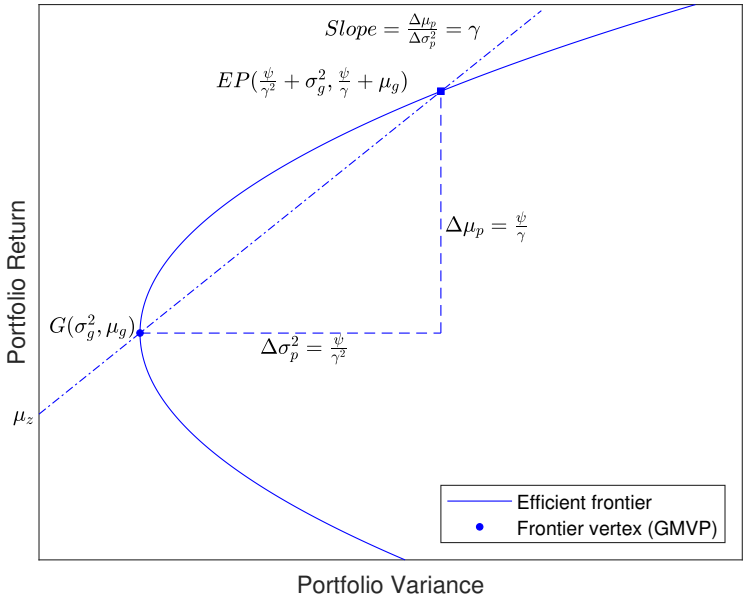


Figure 1. Frontier and risk aversion coefficient. This graph geometrically interprets the risk aversion coefficient (γ) as the marginal reward that an investor needs to take on more risk (in terms of variance) compared to the global minimum variance portfolio (GMVP, with an infinite γ).

Equation (7) highlights two results. First, conditional on ψ, the magnitude of γ depends on the distance between the GMVP's return and the default target return. The higher the value of μ_p, the lower the value of γ. Second, although a higher-degree approximation could obtain a better γ estimation, we restrict our attention to the first- and second-degree Taylor polynomials, as the higher-degree polynomials approach zero as the target return increases. Proposition 1 in Bodnar et al. [29] provided a similar result but a more robust version of γ. Bodnar and Schmid [30,31] also presented relevant estimates of the sample efficient frontier.

3. Estimation of the Risk Aversion Coefficient

When applying the MVU in practice, investors construct portfolios based on their subjective risk aversion coefficient coverage. Such an approach is appropriate if we can ignore the parameter estimates; however, the portfolios make the investment decision unclear due to the estimation risk. For example, Bodnar and Okhrin [11] indicated that the GMVP equivalent has a wider γ confidence interval. This section approximates the γ bounds for non-GMVP-equivalent portfolios based on Equation (7).

3.1. Moments of Sample Efficient Set Constants

Suppose that we form the realized returns r_{it} for N risky assets in T periods, as follows:

$$R = \begin{bmatrix} r_{11} & r_{12} & \cdots & r_{1N} \\ \vdots & \vdots & \ddots & \vdots \\ r_{T1} & r_{T2} & \cdots & r_{TN} \end{bmatrix}. \tag{8}$$

We usually substitute the traditional maximum-likelihood estimates of $\hat{\mu}$ and $\hat{\Sigma}$ into the population efficient set constants:

$$\hat{\mu} = \tfrac{1}{T} R'\ell = \begin{bmatrix} \bar{r}_1 \\ \vdots \\ \bar{r}_N \end{bmatrix} \quad \text{and} \quad \hat{\Sigma} = \tfrac{1}{T}\textstyle\sum_{t=1}^{T} \begin{bmatrix} r_{1t} - \bar{r}_1 \\ \vdots \\ r_{Nt} - \bar{r}_N \end{bmatrix} \begin{bmatrix} r_{1t} - \bar{r}_1 \\ \vdots \\ r_{Nt} - \bar{r}_N \end{bmatrix}' \tag{9}$$

where $\bar{r}_i$ is the sample mean of the ith asset return and $\ell \in \mathbb{R}^T$ denotes the vector of ones.

Assume that the returns are i.i.d. and multivariate normal over time. The following lemma outlines the well-known properties of $\hat{\mu}$ and $\hat{\Sigma}$ (see Muirhead [32], Kan and Zhou [3], Kan and Smith [23]).

Lemma 1. *Under the i.i.d. normality assumption and if $T > N$ (such that Σ is invertible), $\hat{\mu}$ and $\hat{\Sigma}$ are independent of each other and have the following exact distributions:*

$$\hat{\mu} \sim N(\mu, \Sigma/T) \quad \text{and} \quad \hat{\Sigma} \sim W_N(T-1, \Sigma/T) \tag{10}$$

where $W_N(T-1, \Sigma/T)$ denotes an N-dimensional Wishart distribution with $T-1$ degrees of freedom and covariance matrix Σ/T.

We summarize several sample distributions from the studies of Patnaik (1949), Jobson and Korkie [18], Jobson [20], Okhrin and Schmid [22], and Kan and Smith [23] in order to develop an approximate confidence interval for segmenting γ. For reference and simplicity, we use Kan and Smith [23] notation, but replacing $\hat{\psi}^2$ and ψ^2 with $\hat{\psi}$ and ψ, respectively. In addition, we compute the first four raw moments of the singly non-central F-distribution $\hat{\psi}$ based on Patnaik's [33] formulas.

Lemma 2. *Under the assumption of the returns' multivariate normality, assume that $\hat{\psi} \sim (N-1)F_{N-1,T-N+1}(T\psi)/(T-N+1)$; then, the sample's GMVP mean ($\hat{\mu}_g$) conditional on $\hat{\psi}$ is normally distributed, as follows:*

$$\hat{\mu}_g|\hat{\psi} \sim N(\mu_g, \sigma_g^2(1+\hat{\psi})/T) \tag{11}$$

and the sample's GMVP variance ($\hat{\sigma}_g^2$) is distributed as a χ^2-distribution:

$$T\hat{\sigma}_g^2/\sigma_g^2 \sim \chi^2_{T-N}. \tag{12}$$

Additionally, the joint density of $(\hat{\psi}, \hat{\mu}_g, \hat{\sigma}_g^2)$ is provided by

$$f(\hat{\psi}, \hat{\mu}_g, \hat{\sigma}_g^2) = f(\hat{\psi}, \hat{\mu}_g) f(\hat{\sigma}_g^2) = f(\hat{\psi}) f(\hat{\mu}_g|\hat{\psi}) f(\hat{\sigma}_g^2). \tag{13}$$

Moreover, the first few moments of $\hat{\mu}_g$, $\hat{\sigma}_g^2$, and $\hat{\psi}$ are computed as follows:

$$\begin{aligned}
&E(\hat{\mu}_g) = \mu_g, && V(\hat{\mu}_g) = \tfrac{[T(1+\psi)-2]\sigma_g^2}{T(T-N-1)},\\
&E(\hat{\sigma}_g^2) = \tfrac{(T-N)\sigma_g^2}{T}, && V(\hat{\sigma}_g^2) = \tfrac{2(T-N)\sigma_g^4}{T^2},\\
&E(\hat{\psi}) = \tfrac{(T\psi)+N-1}{(T-N-1)}, && E(\hat{\psi}^2) = \tfrac{(T\psi)^2+2(N+1)(T\psi)+(N-1)(N+1)}{(T-N-1)(T-N-3)},\\
&E(\hat{\psi}^3) = \tfrac{(T\psi)^3+3(N+3)(T\psi)^2+3(N+1)(N+3)(T\psi)+(N-1)(N+1)(N+3)}{(T-N-1)(T-N-3)(T-N-5)},\\
&E(\hat{\psi}^4) = \tfrac{(T\psi)^4+4(N+5)(T\psi)^3+6(N+3)(N+5)(T\psi)^2+4(N+1)(N+3)(N+5)(T\psi)}{(T-N-1)(T-N-3)(T-N-5)(T-N-7)}\\
&\qquad\qquad + \tfrac{(N-1)(N+1)(N+3)(N+5)}{(T-N-1)(T-N-3)(T-N-5)(T-N-7)}.
\end{aligned} \tag{14}$$

3.2. GMVP-Equivalent Bounds

Bodnar and Okhrin [11] employed four different tests to determine the GMVP-equivalent bounds, including the GMVP variance, return, return variance, and weight statistics. For brevity, we consider only the first two statistics here. With appropriate

adjustments of the notation, we summarize their bounds at the $(1-\alpha)\times 100$ confidence level as follows:

$$\begin{aligned}\hat{\gamma}_{\chi^2} &= \sqrt{\hat{\mu}'\left[\hat{\Sigma}^{-1}-\frac{\hat{\Sigma}^{-1}\iota'\hat{\Sigma}^{-1}}{\iota'\hat{\Sigma}^{-1}\iota}\right]\hat{\mu}\left(\frac{\chi^2_{T-N;\alpha/2}}{\hat{\sigma}^2_g(T-\chi^2_{T-N;\alpha/2})}\right)} = \sqrt{\frac{\hat{\psi}\chi^2_{T-N;\alpha/2}}{\hat{\sigma}^2_g(T-\chi^2_{T-N;\alpha/2})}},\\ \hat{\gamma}_t &= \frac{\sqrt{T\iota'\hat{\Sigma}^{-1}\iota}}{t_{T-N;1-\alpha/2}}\sqrt{\frac{T-N}{T-1}}\frac{\hat{\mu}'\left[\hat{\Sigma}^{-1}-\frac{\hat{\Sigma}^{-1}\iota'\hat{\Sigma}^{-1}}{\iota'\hat{\Sigma}^{-1}\iota}\right]\hat{\mu}}{\sqrt{1+\frac{T}{T-1}\hat{\mu}'\left[\hat{\Sigma}^{-1}-\frac{\hat{\Sigma}^{-1}\iota'\hat{\Sigma}^{-1}}{\iota'\hat{\Sigma}^{-1}\iota}\right]\hat{\mu}}} = \frac{\hat{\psi}\sqrt{T(T-N)\hat{c}}}{t_{T-N;1-\alpha/2}\sqrt{T-1+T\hat{\psi}}}.\end{aligned} \tag{15}$$

The conditional variable $\hat{\mu}_g|\hat{\psi}$ also provides a conditional statistic for the $\hat{\mu}_g$-γ-equivalent bound:

$$z = \frac{\hat{\mu}_g-\mu_g}{\sqrt{\hat{\sigma}^2_g(1+\hat{\psi})/T}} \Longrightarrow \frac{\hat{\psi}}{\hat{\gamma}}+\hat{\mu}_g \le \hat{\mu}_g + z_{\alpha/2}\sqrt{\frac{1+\hat{\psi}}{T\hat{c}}} \Longrightarrow \hat{\gamma}_z = \frac{\hat{\psi}}{z_{\alpha/2}}\sqrt{\frac{T\hat{c}}{1+\hat{\psi}}}. \tag{16}$$

When the portfolio size and estimation period are kept constant, $\hat{\gamma}_z \ge \hat{\gamma}_t$ generally holds, as $t_{T-N;1-\alpha/2} > z_{\alpha/2}$ is true. It is difficult to compare the GMVP-equivalent bounds expressed in entirely different forms of the χ^2 and z statistics. From a conservative perspective, we name $\hat{\gamma}_g = \max(\hat{\gamma}_{\chi^2}, \hat{\gamma}_t, \hat{\gamma}_z)$ the $\hat{\mu}_g$-γ-equivalent bound.

3.3. Estimation of the Risk Aversion Coefficient

Equation (7) expresses γ in terms of an infinite series, but the efficient set constants are not directly observable. Consider the plug-in $\hat{\gamma}$ as a proxy of γ:

$$\hat{\gamma} = \frac{\hat{\psi}}{\mu_p}\left[1+\left(\frac{\hat{\mu}_g}{\mu_p}\right)+\left(\frac{\hat{\mu}_g}{\mu_p}\right)^2+\cdots\right] \tag{17}$$

where $\hat{a} = \hat{\mu}'\hat{\Sigma}^{-1}\hat{\mu}$, $\hat{b} = \iota'\hat{\Sigma}^{-1}\hat{\mu}$, $\hat{c} = \iota'\hat{\Sigma}^{-1}\iota$, and $\hat{\psi}$ are the sample mappings of a, b, c, and ψ, respectively.

Under the normality of returns, Equation (11) shows that the sample's GMVP mean ($\hat{\mu}_g$) conditional on $\hat{\psi}$ has the following conditional probability density function:

$$f(\hat{\mu}_g|\hat{\psi}) = \frac{1}{\sqrt{\frac{2\pi\sigma^2_g(1+\hat{\psi})}{T}}}\,exp\left[-\frac{\left(\hat{\mu}_g-\mu_g\right)^2}{\frac{2\sigma^2_g(1+\hat{\psi})}{T}}\right]. \tag{18}$$

Thus, $\hat{\gamma} = \frac{\hat{\psi}}{\mu_p-\hat{\mu}_g}$ has the following conditional probability density function:

$$f(\hat{\gamma}|\hat{\psi}) = \frac{\hat{\psi}^2}{\hat{\gamma}^2\sqrt{\frac{2\pi\sigma^2_g(1+\hat{\psi})}{T}}}\,exp\left[-\frac{\left(\mu_p-\frac{\hat{\psi}}{\hat{\gamma}}-\mu_g\right)^2}{\frac{2\sigma^2_g(1+\hat{\psi})}{T}}\right]. \tag{19}$$

Finally, the marginal distribution of $\hat{\gamma}$ can be expressed as an integral, as follows:

$$f(\hat{\gamma}) = \int_0^\infty \frac{\hat{\psi}^2}{\hat{\gamma}^2\sqrt{\frac{2\pi\sigma^2_g(1+\hat{\psi})}{T}}}\,exp\left[-\frac{\left(\mu_p-\frac{\hat{\psi}}{\hat{\gamma}}-\mu_g\right)^2}{\frac{2\sigma^2_g(1+\hat{\psi})}{T}}\right]p(\hat{\psi})\,d\hat{\psi} \tag{20}$$

where

$$p(\hat{\psi}) = \sum_{k=0}^{\infty}\frac{\Gamma\left(\frac{T}{2}+k\right)e^{-T\psi/2}\left(\frac{T\psi}{2}\right)^k}{\Gamma\left(\frac{T-N+1}{2}\right)\Gamma\left(\frac{N-1}{2}+k\right)k!}\left(\frac{T-N+1}{(T-N+1)+(N-1)\hat{\psi}}\right)^{\frac{T}{2}+k}\hat{\psi}^{\frac{N-3}{2}+k}. \tag{21}$$

Instead of deriving the exact distribution of the estimated risk aversion coefficient, the expected value of $\hat{\gamma}$ does not exist:

$$E(\hat{\gamma}) = E\big(E(\hat{\gamma}|\hat{\psi})\big) = \infty \tag{22}$$

where the inverse moment of a normal random variable approaches infinity due to a singularity at μ_g:

$$\begin{aligned} E(\hat{\gamma}|\hat{\psi}) &= \int_{-\infty}^{\infty} \frac{\hat{\psi}^2}{|\hat{\gamma}|\sqrt{\frac{2\pi\sigma_g^2(1+\hat{\psi})}{T}}} exp\left[-\frac{\left(\mu_p - \frac{\hat{\psi}}{\hat{\gamma}} - \mu_g\right)^2}{\frac{2\sigma_g^2(1+\hat{\psi})}{T}}\right] d\hat{\gamma} \\ &= \hat{\psi}\int_{-\infty}^{\infty} |\mu_p - \hat{\mu}_g| f(\hat{\mu}_g|\hat{\psi})\, d\hat{\mu}_g \\ &= \infty. \end{aligned} \tag{23}$$

As the inverse moment of the conditional normal random variable $\hat{\mu}_g|\hat{\psi}$ does not exist, the moments of $\hat{\gamma}$ provide no inference to segment the μ_p-equivalent. However, the Taylor expansion in Equation (17) can express the risk aversion coefficient. This study only considers the plug-in first- and second-degree formulas for γ:

$$\begin{aligned} \hat{\gamma}_1 &= \frac{\hat{\psi}}{\mu_p}\left[1 + \left(\frac{\hat{\mu}_g}{\mu_p}\right)\right], \\ \hat{\gamma}_2 &= \frac{\hat{\psi}}{\mu_p}\left[1 + \left(\frac{\hat{\mu}_g}{\mu_p}\right) + \left(\frac{\hat{\mu}_g}{\mu_p}\right)^2\right] = \hat{\gamma}_1 + \hat{\gamma}_e. \end{aligned} \tag{24}$$

We do not approximate γ via different Taylor expansions of the estimated γ; our main purpose is only to use their "approximated confidence intervals" as tools to segment $\hat{\gamma}$. Equipped with Lemma 1 and Lemma 2, the following results provide the first two moments of $\hat{\gamma}_1$ and $\hat{\gamma}_2$.

Theorem 2. *Given a target return μ_p, the plug-in estimators $\hat{\gamma}_1$ and $\hat{\gamma}_2$ have the following expected values:*

$$\begin{aligned} E(\hat{\gamma}_1) &= \frac{1}{\mu_p}\left(E(\hat{\psi}) + \frac{E(\hat{\psi}\hat{\mu}_g)}{\mu_p}\right) = E(\hat{\psi})\left(\frac{1}{\mu_p} + \frac{\mu_g}{\mu_p^2}\right), \\ V(\hat{\gamma}_1) &= \frac{V(\hat{\psi})T^2(\mu_p+\mu_g)^2 + E(\hat{\psi}^2)(T-N)\sigma_g^2 + E(\hat{\psi}^3)(T-N)\sigma_g^2}{T^2\mu_p^4}, \end{aligned} \tag{25}$$

and

$$\begin{aligned} E(\hat{\gamma}_2) &= E(\hat{\psi})\left(\frac{1}{\mu_p} + \frac{\mu_g}{\mu_p^2} + \frac{\mu_g^2}{\mu_p^3} + \frac{\sigma_g^2(T-N)}{T^2\mu_p^3}\right) + E(\hat{\psi}^2)\left(\frac{\sigma_g^2(T-N)}{T^2\mu_p^3}\right), \\ V(\hat{\gamma}_2) &= V(\hat{\gamma}_1) + \frac{E(\hat{\psi}^2\hat{\mu}_g^4) - \left(E(\hat{\psi}\hat{\mu}_g^2)\right)^2}{\mu_p^6} \\ &\quad + 2\left[\frac{E(\hat{\psi}^2\hat{\mu}_g^2)}{\mu_p^4} + \frac{E(\hat{\psi}^2\hat{\mu}_g^3)}{\mu_p^5} - \left(\frac{E(\hat{\psi})}{\mu_p} + \frac{E(\hat{\psi}\hat{\mu}_g)}{\mu_p^2}\right)\left(\frac{E(\hat{\psi}\hat{\mu}_g^2)}{\mu_p^3}\right)\right]. \end{aligned} \tag{26}$$

For the proof, see Appendix A.

Equations (25) and (26) have two implications. First, $\hat{\gamma}_1$ and $\hat{\gamma}_2$ are biased estimators that underestimate the exact γ. However, the gains in computation for a higher target return μ_p and the derivations of the higher-order moments are evident. Bodnar and Okhrin [11] have statistically demonstrated the bound of γ for the GMVP-equivalents. Therefore, we merely need to resolve the confidence intervals for the non-GMVP-equivalents that have a higher μ_p with a lower γ. In this situation, the ratio $\hat{\mu}_g/\mu_p$ becomes sufficiently small; thus, the higher-degree remainders approach zero such that the estimates $\hat{\gamma}$, $\hat{\gamma}_1$, and $\hat{\gamma}_2$ are very close. Moreover, although the difference between $\hat{\gamma}_1$ and $\hat{\gamma}_2$ may be dramatic at lower target returns, the conclusion holds outside the $\hat{\mu}_g$-γ-equivalents.

Second, given a particular target return μ_p^*, Equation (25) yields the first-degree estimate $\hat{\gamma}_1^*$. As the historical data used here generally consist of long time-series, we can establish the asymptotically normal confidence interval for the risk aversion coefficient:

$$\left[\hat{\gamma}_1^* - z_{\alpha/2}\sqrt{V(\hat{\gamma}_1^*)}, \hat{\gamma}_1^* + z_{\alpha/2}\sqrt{V(\hat{\gamma}_1^*)}\right]. \tag{27}$$

Taking the condition $\mu_p > \mu_g > 0$ and the feature of $\hat{\gamma} > \hat{\gamma}_1$ into account, we obtain the first-degree approximate μ_p^*-γ-equivalents:

$$[L^*, U^*] = \left[\hat{\gamma}_1^*, \hat{\gamma}_1^* + z_{\alpha/2}\sqrt{V(\hat{\gamma}_1^*)}\right]. \tag{28}$$

Likewise, considering the condition $\mu_p > \mu_g > 0$ and the property $\hat{\gamma} > \hat{\gamma}_2$, the second-degree approximate μ_p^*-γ-equivalent interval relative to μ_p^* is provided by

$$[L^*, U^*] = \left[\hat{\gamma}_2^*, \hat{\gamma}_2^* + z_{\alpha/2}\sqrt{V(\hat{\gamma}_2^*)}\right]. \tag{29}$$

3.4. Segmenting Investment Opportunities

This section consists of two parts: segmenting the sample frontier (with the vertical return axis) and extending it to other mean-variance investment opportunities (with the horizontal variance axis).

Figure 2 demonstrates the first part of segmenting the sample frontier via the first-degree $\hat{\mu}_p$-γ-equivalent interval. We use the $\hat{\gamma}_g$ of the GMVP as our starting point to build a non-overlapping interval $[L_1, U_1]$ for a particular μ_p at the $(1-\alpha)\times 100$ confidence level which connects the GMVP-equivalent bound. We first require the horizontal line through $\hat{\gamma}_g$ to intersect the upper bound curve of $\hat{\gamma}_1$ at the location U_1, that is, the $\hat{\gamma}_g$ of the GMVP should equal the upper limit of the interval $[L_1, U_1]$ given the target return μ_{p_1}:

$$U_1 = \frac{\hat{\psi}\mu_p + \hat{\psi}\mu_g}{\mu_p^2} + z_{\alpha/2}\sqrt{\frac{V(\hat{\psi})T^2(\mu_p+\mu_g)^2}{T^2\mu_p^4} + \frac{E(\hat{\psi}^2)(T-N)\sigma_g^2}{T^2\mu_p^4} + \frac{E(\hat{\psi}^3)(T-N)\sigma_g^2}{T^2\mu_p^4}} = \hat{\gamma}_g. \tag{30}$$

Rearranging Equation (30) with respect to the variable μ_p, we obtain the following fourth-order equation:

$$\begin{cases} a_4\mu_p^4 + a_3\mu_p^3 + a_2\mu_p^2 + a_1\mu_p + a_0 = 0, \\ a_4 = T^2\hat{\gamma}_g^2, \\ a_3 = -2T^2\hat{\gamma}_g\hat{\psi}, \\ a_2 = T^2\hat{\psi}^2 - 2T^2\hat{\gamma}_g\hat{\psi}\hat{\mu}_g - z_{\alpha/2}^2 V(\hat{\psi})T^2, \\ a_1 = 2T^2\hat{\psi}^2\hat{\mu}_g - 2z_{\alpha/2}^2 T^2 V(\hat{\psi})\hat{\mu}_g, \\ a_0 = T^2\hat{\psi}^2\hat{\mu}_g^2 - z_{\alpha/2}^2\Big(T^2 V(\hat{\psi})\hat{\mu}_g^2 + E(\hat{\psi}^2)(T-N)\hat{\sigma}_g^2 + E(\hat{\psi}^3)(T-N)\hat{\sigma}_g^2\Big). \end{cases} \tag{31}$$

Through either a closed-form solution or a numerical method, Figure 2 denotes μ_{p_1}, which is the desired target return when solving Equation (31). Substituting μ_{p_1} into Equation (30), we obtain the corresponding first-degree approximation $L_1 = \hat{\gamma}_1$ and the μ_{p_1}-γ-equivalent interval $[L_1, U_1]$. All the portfolios with $\gamma \in [L_1, U_1]$ are statistically equivalent to the efficient portfolio with the risk aversion coefficient L_1 (or the target portfolio μ_{p_1}). As a result, we obtain three isomorphic hierarchies of μ_p-γ-equivalents, including μ_g, μ_{p_1}; in addition, the remaining target returns are higher than μ_{p_1}. We obtain the second μ_{p_2}-γ-equivalent interval $[L_2, U_2]$ by using L_1 as the next starting point and repeating the same procedure. If we successively repeat this process k times, we can segment the frontier into $k+2$ isomorphic hierarchies of μ_p-γ-equivalents.

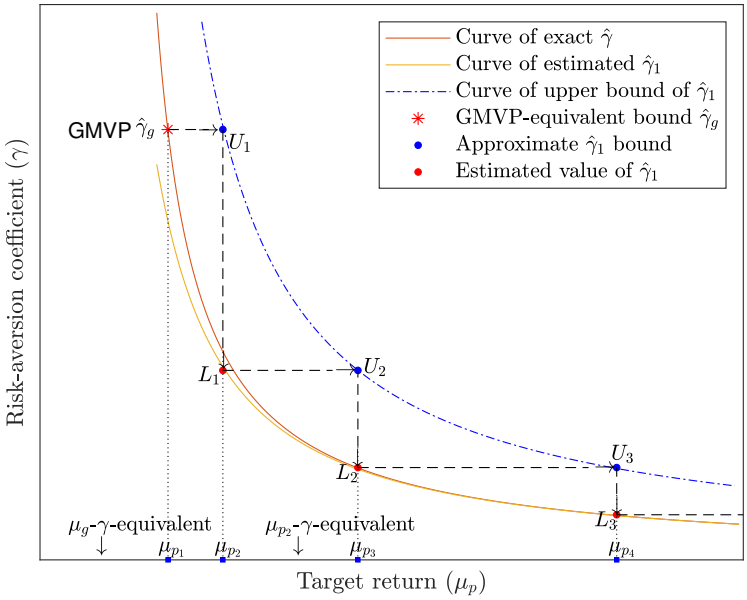


Figure 2. Procedure for constructing μ_p-γ-equivalents. This graph plots the construction of first-degree non-overlapping $\hat{\mu}_p$-γ-equivalent intervals. The GMVP-equivalent bound $\hat{\gamma}_g$ yields an interval $\gamma_1 \in [L_1, U_1]$ for a particular target return μ_{p_1} at the $(1-\alpha)\times 100$ confidence level to connect the GMVP-equivalent. We name $[L_1, U_1]$ the μ_{p_1}-γ-equivalent. Likewise, using L_1 as the next starting point and repeating the same procedures yields the μ_{p_2}-γ-equivalent interval $[L_2, U_2]$.

Holding the confidence level, portfolio size, and estimation period constant, we can apply a similar analysis to the second-degree approximation $\hat{\gamma}_2$:

$$\left(\frac{\hat{\psi}\mu_p^2+\hat{\psi}\hat{\mu}_g\mu_p+\hat{\psi}\hat{\mu}_g^2-\hat{\gamma}_g\mu_p^3}{\mu_p^3}\right)^2 = z_{\alpha/2}^2\left[\left(\frac{E(\hat{\psi}^2\hat{\mu}_g^2)-E(\hat{\psi})E(\hat{\psi}\hat{\mu}_g^2)}{\mu_p^4}+\frac{E(\hat{\psi}^2\hat{\mu}_g^3)-E(\hat{\psi}\hat{\mu}_g)E(\hat{\psi}\hat{\mu}_g^2)}{\mu_p^5}\right)\right.$$
$$\left.+\frac{V(\hat{\psi})T^2(\mu_p+\hat{\mu}_g)^2+E(\hat{\psi}^2)(T-N)\hat{\sigma}_g^2+E(\hat{\psi}^3)(T-N)\hat{\sigma}_g^2}{T^2\mu_p^4}+\frac{E(\hat{\psi}^2\hat{\mu}_g^4)-\left(E(\hat{\psi}\hat{\mu}_g^2)\right)^2}{\mu_p^6}\right]. \tag{32}$$

Then, we can successively repeat this process to segment the frontier into isomorphic hierarchies of μ_p-γ-equivalents. The only difference is that we need to solve the following sixth-order equation concerning the variable μ_p using a numerical method:

$$\begin{cases} a_6\mu_p^6+a_5\mu_p^5+a_4\mu_p^4+a_3\mu_p^3+a_2\mu_p^2+a_1\mu_p+a_0=0, \\ a_6 = T^2\hat{\gamma}_g^2, \\ a_5 = -2T^2\hat{\gamma}_g\hat{\psi}, \\ a_4 = T^2\hat{\psi}^2-2T^2\hat{\gamma}_g\hat{\psi}\hat{\mu}_g-z_{\alpha/2}^2T^2V(\hat{\psi}), \\ a_3 = 2T^2\hat{\psi}^2\hat{\mu}_g-2T^2\hat{\gamma}_g\hat{\psi}\hat{\mu}_g^2-2z_{\alpha/2}^2V(\hat{\psi})T^2\hat{\mu}_g, \\ a_2 = 3T^2\hat{\psi}^2\hat{\mu}_g^2-2z_{\alpha/2}^2T^2\left(E(\hat{\psi}^2\hat{\mu}_g^2)-E(\hat{\psi})E(\hat{\psi}\hat{\mu}_g^2)\right) \\ \qquad -z_{\alpha/2}^2\left(V(\hat{\psi})T^2\hat{\mu}_g^2+E(\hat{\psi}^2)(T-N)\hat{\sigma}_g^2+E(\hat{\psi}^3)(T-N)\hat{\sigma}_g^2\right), \\ a_1 = 2T^2\hat{\psi}^2\hat{\mu}_g^3-2z_{\alpha/2}^2T^2\left(E(\hat{\psi}^2\hat{\mu}_g^3)-E(\hat{\psi}\hat{\mu}_g)E(\hat{\psi}\hat{\mu}_g^2)\right), \\ a_0 = T^2\hat{\psi}^2\hat{\mu}_g^4-z_{\alpha/2}^2T^2\left(E(\hat{\psi}^2\hat{\mu}_g^4)-\left(E(\hat{\psi}\hat{\mu}_g^2)\right)^2\right). \end{cases} \tag{33}$$

The second part includes other investment opportunities using the horizontal variance axis. Specifically, we construct the approximate upper confidence limit of the sample variance $\hat{\sigma}_p^2$. Proposition 2 of Kan and Smith [23], with a notation adjustment, provides a distribution of the sample mean-variance frontier under certain conditions, which helps to accomplish this task.

Lemma 3. *For the sample minimum-variance portfolio ω_p and given a target return of μ_p, the sample distribution of $\hat{\sigma}_p^2$ is distributed as*

$$\frac{T\hat{\sigma}_p^2}{\sigma_g^2\left(1+\frac{y^2}{u}\right)} \sim \chi^2_{T-N+1}, \tag{34}$$

where $u \sim \chi^2_{T-N+1}(T\psi)$ and $y \sim N(\sqrt{T}(\mu_p-\mu_g)/\sigma_g, 1)$.

For simplicity, we consider the denominator's random variable $\sigma_g^2(1+y^2/u)$ as a proxy of the parameter σ_p^2 in Equation (34). As the sample frontier is considered a proxy of the population frontier, we only need an upper confidence limit of σ_p^2 for a particular μ_p at the $(1-\alpha)\times 100$ confidence level:

$$\left[\hat{\sigma}_p^2, \frac{T\hat{\sigma}_p^2}{\chi^2_{T-N+1;\alpha/2}}\right]. \tag{35}$$

Kan and Smith provided the exact distribution of $\hat{\sigma}_p^2$, whereas our approach only approximates the confidence limit of σ_p^2. By integrating Equations (28)–(33) (the vertical return axis) and Equation (35) (the horizontal variance axis), we can segment the mean-variance portfolios in a hierarchy based on the μ_p-σ_p^2-γ-equivalent areas.

4. Illustration

In this section, we itemize the μ_p-σ_p^2-γ-equivalents relative to particular target returns at various horizons and the related isomorphic hierarchy of risk aversion coefficients. The complete set of assets consisted of the DJIA stocks and the United States 10-year bond yield. We are grateful to Yahoo Finance and Investing for providing their historical data on their websites https://www.finance.yahoo.finance.com (accessed on 10 September 2024) and https://www.investing.com/rates-bonds/u.s.-10-year-bond-yield-historical-data (accessed on 10 September 2024), respectively. Using this asset set instead of randomly simulating stocks has three advantages: first, the DJIA 29 firms are composed of the appropriate assets set, home to giants such as Apple, Nike, and Walmart; thus, our results are not driven by the small-firm effect and small portfolio sizes. In this regard, Tang [34] summarized the optimal number of assets for diversification as falling between 8 and 40. Second, investors typically utilize changes in the United States 10-year bond yield to analyze global market sentiment and the economic landscape. Third, as shown later, the estimated γ domains fit the range that is commonly used in practice.

4.1. Data

The sample consisted of weekly returns of the 29 DJIA stocks and the United States 10-year bond yield. The evaluation ranged from January 2011 to December 2020, and the rolling window had sizes of three and five years. All 3-year estimates used all 29 stocks (or the 29 stocks plus bonds). Meanwhile, the 5-year estimates for 2011–2012 only used 28 stocks (or the 28 stocks plus bonds).

We present four different γ estimators by combining the approximation method and the assets set (with or without bonds). The estimate $\hat{\gamma}_{1A}$ ($\hat{\gamma}_{2A}$) denotes the first-degree (second-degree) approximation using the DJIA stocks exclusively. Additionally, the estimate $\hat{\gamma}_{1B}$ ($\hat{\gamma}_{2B}$) denotes the first-degree (second-degree) approximation containing both the DJIA stocks and United States 10-year bonds.

4.2. Estimated GMVP-Equivalent Bounds

The μ_p-γ-equivalent constructions proposed above require specification of the GMVP-equivalent γ bound in Equations (15) and (16). Table 1 reports the estimated GMVP-equivalent bounds at the 95% confidence level using only the DJIA risky assets, while

Table 2 reports the estimated GMVP-equivalent bounds at the 95% confidence level using both the DJIA risky assets and the United States 10-year bonds.

Table 1. Estimated GMVP-equivalent bounds of stocks only. This table estimates the parameters at the 95% confidence level ($\delta = 5\%$). The set of assets contains the DJIA stocks only. The GMVP-equivalent bounds of the χ^2-statistics and t-statistics were computed based on Equation (15). The z-statistics were calculated using Equation (16), and provide more conservative bounds compared to the other statistics.

		Three-Year Estimation			Five-Year Estimation		
Year		$\hat{\gamma}$	**Return**	**Variance**	$\hat{\gamma}$	**Return**	**Variance**
2011	GMVP		0.002248	0.000197		0.002174	0.000318
	χ^2-statistic	34.3722	0.006298	0.000315	24.5131	0.004946	0.000432
	t-statistic	53.0117	0.004874	0.000247	28.5939	0.004550	0.000402
	z-statistic	59.1503	0.004602	0.000237	30.3661	0.004412	0.000392
2012	GMVP		0.001735	0.000155		0.001635	0.000294
	χ^2-statistic	37.7067	0.005193	0.000246	22.0166	0.003931	0.000398
	t-statistic	56.5323	0.004042	0.000196	22.3370	0.003898	0.000395
	z-statistic	63.0278	0.003804	0.000188	23.7207	0.003766	0.000384
2013	GMVP		0.002417	0.000157		0.002521	0.000191
	χ^2-statistic	39.2174	0.006073	0.000251	31.3315	0.004685	0.000260
	t-statistic	61.3090	0.004756	0.000195	36.7618	0.004365	0.000241
	z-statistic	68.3555	0.004515	0.000188	39.1251	0.004254	0.000235
2014	GMVP		0.002496	0.000128		0.002290	0.000161
	χ^2-statistic	50.1698	0.006305	0.000204	34.6093	0.004309	0.000220
	t-statistic	88.6955	0.004651	0.000152	41.1818	0.003987	0.000203
	z-statistic	98.9008	0.004428	0.000148	43.8294	0.003884	0.000198
2015	GMVP		0.002355	0.000154		0.002200	0.000179
	χ^2-statistic	54.1807	0.007346	0.000247	43.8273	0.005030	0.000243
	t-statistic	110.2530	0.004808	0.000177	67.7737	0.004030	0.000206
	z-statistic	123.0559	0.004553	0.000172	72.1372	0.003919	0.000202
2016	GMVP		0.001054	0.000164		0.001939	0.000164
	χ^2-statistic	35.8846	0.004573	0.000262	41.1920	0.004388	0.000224
	t-statistic	53.0141	0.003436	0.000209	58.0539	0.003677	0.000194
	z-statistic	59.1510	0.003189	0.000200	61.7894	0.003572	0.000191
2017	GMVP		0.001725	0.000129		0.002367	0.000142
	χ^2-statistic	49.6423	0.005554	0.000206	52.1803	0.005062	0.000194
	t-statistic	87.5251	0.003897	0.000154	85.2631	0.004016	0.000162
	z-statistic	97.6720	0.003671	0.000149	90.7783	0.003916	0.000159
2018	GMVP		0.001939	0.000197		0.001716	0.000205
	χ^2-statistic	36.2179	0.006171	0.000314	41.0287	0.004758	0.000279
	t-statistic	58.2822	0.004569	0.000242	63.6355	0.003677	0.000236
	z-statistic	64.9824	0.004298	0.000233	67.7327	0.003558	0.000232
2019	GMVP		0.003835	0.000183		0.002469	0.000199
	χ^2-statistic	45.8556	0.008813	0.000292	41.0551	0.005429	0.000272
	t-statistic	87.2492	0.006451	0.000213	62.9210	0.004400	0.000230
	z-statistic	97.2959	0.006181	0.000207	66.9719	0.004283	0.000227
2020	GMVP		0.003426	0.000379		0.002705	0.000309
	χ^2-statistic	25.3883	0.009122	0.000603	31.9398	0.006271	0.000421
	t-statistic	39.8354	0.007056	0.000470	47.5510	0.005100	0.000359
	z-statistic	44.4140	0.006682	0.000452	50.6117	0.004955	0.000353

Several observations can be made based on Tables 1 and 2. First, Tables 1 and 2 show that the z-statistics provide a more conservative bound for γ than those using t-statistics across years and horizons. Second, adding the Visa stock to the assets set (5-year estimates in 2013–2020) yields a more conservative γ bound than those outside the breaking point. Table 1 indicates that the 5-year γ estimates without the Visa stock moved from 22.0166–30.3661 in 2011–2012 to 31.3315–90.7783 in 2013–2020. Moreover, Table 2 reports

the same effect observed in Table 1. Meanwhile, each matched comparison between Tables 1 and 2 indicates that the portfolios with bonds have a more conservative γ bound than those without bonds. Finally, as mentioned by Bodnar and Okhrin, γ usually ranges between 1 and 50 in empirical applications. In Tables 1 and 2, almost half of the 5-year estimates satisfy this condition. The remaining GMVP-equivalent γ bounds are higher than 50. These γ ranges are wide enough for us to segment the sample frontier.

Table 2. Estimated GMVP-equivalent bounds including bonds. This table estimates the parameters at the 95% confidence level ($\delta = 5\%$). The set of assets contains the DJIA stocks and the corresponding United States 10-year bond yield. The GMVP-equivalent bounds of the χ^2-statistics and t-statistics were computed based on Equation (15), while the z-statistics used Equation (16).

		Three-Year Estimation			Five-Year Estimation		
Year		$\hat{\gamma}$	**Return**	**Variance**	$\hat{\gamma}$	**Return**	**Variance**
2011	GMVP		0.001758	0.000181		0.001930	0.000284
	χ^2-statistic	37.2926	0.005894	0.000292	26.0435	0.004606	0.000387
	t-statistic	60.6220	0.004302	0.000223	30.9500	0.004181	0.000357
	z-statistic	67.9174	0.004029	0.000215	32.9398	0.004045	0.000348
2012	GMVP		0.001720	0.000146		0.001254	0.000243
	χ^2-statistic	38.3330	0.005122	0.000235	24.6640	0.003419	0.000331
	t-statistic	57.9339	0.003971	0.000185	25.8604	0.003319	0.000323
	z-statistic	64.8491	0.003731	0.000177	27.5222	0.003195	0.000313
2013	GMVP		0.002408	0.000153		0.002248	0.000181
	χ^2-statistic	39.2551	0.006061	0.000246	33.5794	0.004480	0.000247
	t-statistic	61.8598	0.004726	0.000191	41.5663	0.004051	0.000224
	z-statistic	69.2458	0.004479	0.000183	44.3357	0.003939	0.000219
2014	GMVP		0.002555	0.000125		0.002311	0.000156
	χ^2-statistic	50.3923	0.006367	0.000200	34.8884	0.004317	0.000214
	t-statistic	89.9932	0.004689	0.000148	41.8180	0.003984	0.000196
	z-statistic	100.7499	0.004461	0.000144	44.6038	0.003880	0.000191
2015	GMVP		0.002275	0.000152		0.002113	0.000171
	χ^2-statistic	54.2063	0.007322	0.000245	44.5437	0.004920	0.000234
	t-statistic	111.6907	0.004724	0.000174	69.6026	0.003910	0.000197
	z-statistic	125.1646	0.004461	0.000170	74.2459	0.003797	0.000194
2016	GMVP		0.001181	0.000159		0.001988	0.000159
	χ^2-statistic	36.4785	0.004726	0.000256	41.5658	0.004426	0.000218
	t-statistic	54.8948	0.003537	0.000202	59.1013	0.003703	0.000188
	z-statistic	61.4972	0.003284	0.000193	63.0417	0.003596	0.000185
2017	GMVP		0.001777	0.000125		0.002353	0.000140
	χ^2-statistic	49.9492	0.005597	0.000202	52.2279	0.005047	0.000191
	t-statistic	88.8992	0.003924	0.000149	85.9338	0.003991	0.000159
	z-statistic	99.6061	0.003693	0.000144	91.6931	0.003888	0.000156
2018	GMVP		0.001849	0.000183		0.001617	0.000194
	χ^2-statistic	37.1890	0.005986	0.000295	41.9842	0.004611	0.000265
	t-statistic	60.4208	0.004396	0.000225	65.7532	0.003529	0.000223
	z-statistic	67.6367	0.004124	0.000217	70.1398	0.003409	0.000219
2019	GMVP		0.003230	0.000167		0.002231	0.000186
	χ^2-statistic	49.7536	0.008267	0.000268	42.8795	0.005161	0.000254
	t-statistic	99.0771	0.005760	0.000192	67.1462	0.004102	0.000214
	z-statistic	110.9335	0.005489	0.000187	71.6256	0.003985	0.000210
2020	GMVP		0.002884	0.000309		0.002689	0.000280
	χ^2-statistic	28.1763	0.008166	0.000496	33.2586	0.006114	0.000383
	t-statistic	45.1224	0.006183	0.000382	49.8493	0.004974	0.000326
	z-statistic	50.5107	0.005831	0.000367	53.1739	0.004831	0.000320

4.3. Example

This study employs the GMVP-equivalent bound as the highest risk aversion coefficient (M). Following the common practice of assigning γ (from 1 to M), we define the

domain of γ as $[L, M]$ in order to successfully solve the isomorphic hierarchies problem. The first μ_p-γ-equivalent interval chooses its upper limit, which is equal to the GMVP-equivalent bound. In each successive step, we construct non-overlapping μ_p-γ-equivalent intervals until a specific lower limit (L) is reached such that its value is the nearest to and less than one and $\gamma = 1 \in [L, M]$. Figure 3 presents an isomorphic hierarchy with five tiers based on the 5-year approximation $\hat{\gamma}_{1A} \in [0.9230, 39.1251]$ for 2013. This γ domain fits the requirement of Bodnar and Okhrin. As highlighted in Figure 3, the results show that isomorphic hierarchies of risk aversion coefficients are better than traditional isometric attributes.

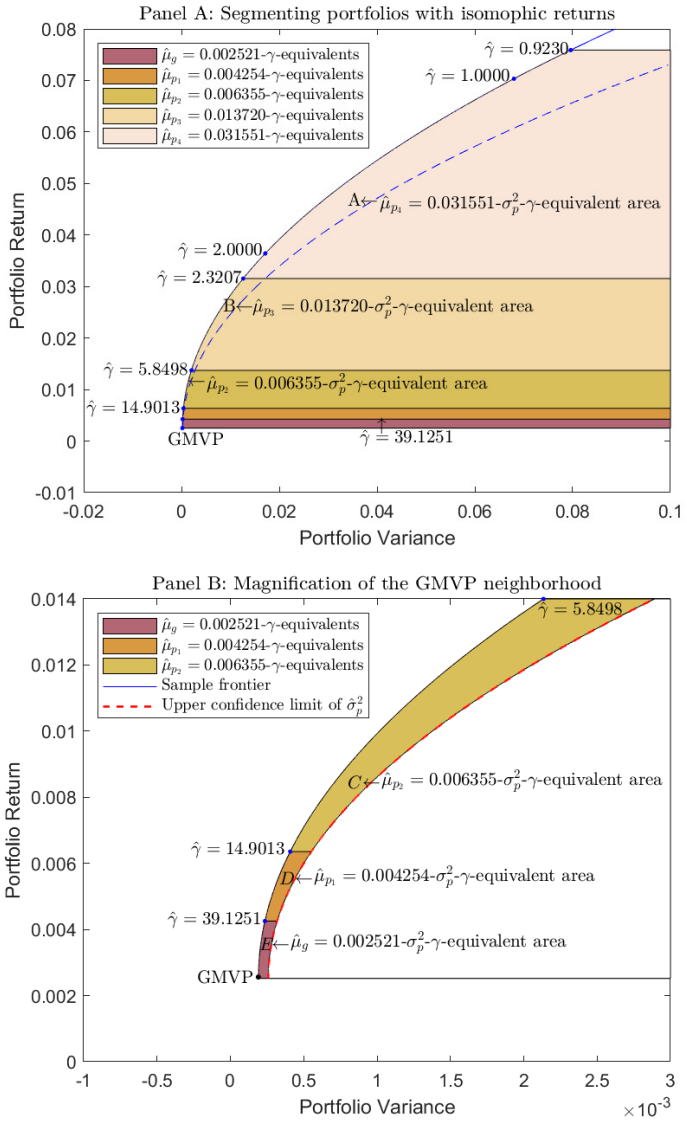


Figure 3. Five years isomorphic tiers in 2013. Panel (**A**) illustrates the isomorphic tiers of the risk aversion coefficients using different shaded areas, with darker colors indicating higher risk aversion coefficients and lower thickness implying a shorter γ interval. Panel (**B**) specifically magnifies the GMVP neighborhood with $\hat{\gamma}_{1A} \geq 40$. The values $\hat{\gamma}_{1A} = 15, 16, \ldots, 39$ cluster around the $\hat{\mu}_{p_1}$-γ-equivalent, $\hat{\gamma}_{1A} = 6, 7, \ldots, 15$ fall inside the $\hat{\mu}_{p_2}$-γ-equivalent, the $\hat{\mu}_{p_3}$-γ-equivalent contains $\hat{\gamma}_{1A} = 3, 4, 5$, and the $\hat{\mu}_{p_4}$-γ-equivalent only contains the lower risk aversion coefficients $\hat{\gamma}_{1A} = 1, 2$.

Many portfolios may be μ_p-γ-equivalent at the 5% level. The classification of mean-variance portfolios starts with the $\hat{\mu}_g = 0.002521$-γ-equivalent, where the portfolio returns range from 0.002521 to 0.004254 (with $\hat{\gamma}_{1A} > 39.1251$); this tier is narrower than the others. The second tier is the $\hat{\mu}_{p_1} = 0.004254$-$\gamma$-equivalents, where the portfolio returns and

risk aversion coefficients are $0.004254 \leq r_p < 0.006355$ and $39.1251 \geq \hat{\gamma}_{1A} > 14.9013$, respectively. The following tier proceeds in a similar manner, ending at the $\hat{\mu}_{p_5} = 0.031551$-$\gamma$-equivalents (with $0.9230 < \hat{\gamma}_{1A} \leq 2.3207$). In contrast, we observe that most of the values of $\hat{\gamma}_{1A} = 15, 16, \ldots, 39$ cluster around the $\hat{\mu}_{p_1}$-γ-equivalent, $\hat{\gamma}_{1A} = 6, 7, \ldots, 15$ fall inside the $\hat{\mu}_{p_2}$-γ-equivalent, the $\hat{\mu}_{p_3}$-γ equivalent contains $\hat{\gamma}_{1A} = 3, 4, 5$, and the $\hat{\mu}_{p_4}$-γ-equivalent only contains the lower risk aversion coefficients $\hat{\gamma}_{1A} = 1, 2$. Next, we use Equation (35) to approximate the confidence limit of σ_p^2 according to the vertical return axis. The area bounded by the sample frontier and upper confidence limit is the μ_p-σ_p^2-γ-equivalent portfolio.

4.4. Tiers of Risk Aversion Coefficients

We also examine the tiers of the μ_p-γ-equivalents across years and horizons. Let $Tier_{1A}$, $Tier_{1B}$, $Tier_{2A}$, and $Tier_{2B}$ denote the isomorphic hierarchy tiers of γ according to the estimates $\hat{\gamma}_{1A}$, $\hat{\gamma}_{1B}$, $\hat{\gamma}_{2A}$, and $\hat{\gamma}_{2B}$, respectively. Table 3 reports the tier variations in 30 matched comparisons (grouped by year and horizon), where the majority are 80% indifferent tiers (24 in 30 matched comparisons):

$$Tier_{1A} = Tier_{1B} = Tier_{2A} = Tier_{2B}. \tag{36}$$

Table 3 also details the representation of potential variations that may arise from three sources. The first is mainly the 5% matched comparison, which is due to the approximation effect (the 5-year estimation in 2015).

$$Tier_1 \neq Tier_2 \text{ (or } Tier_{1A} = Tier_{1B} \neq Tier_{2A} = Tier_{2B}) \tag{37}$$

$$Tier_A \neq Tier_B \text{ (or } Tier_{1A} = Tier_{2A} \neq Tier_{1B} = Tier_{2B}) \tag{38}$$

Figure 4 plots the approximation effect, in which the tiers obtained using the first-degree approximation (the left panel) are different from those based on the second-degree approximation (the right panel). The second 5% matched comparison comes from the effect of the assets set (the 5-year estimate in 2013). Figure 5 depicts the corresponding impact, where the tiers based exclusively on stocks (the top panel) are different from those containing stocks and bonds (the bottom panel).

Finally, the 10% matched comparisons may have a mixed effect on the approximation and assets (i.e., the 5-year estimate in 2012 and the 5-year estimate in 2019). Figure 6 shows that the bottom-right estimate $Tier_{2B}$ (42) has a significantly different lower limit among the four calculations:

$$Tier_{1B} = Tier_{2A} = Tier_{2B} \neq Tier_{1A}, \tag{39}$$

$$Tier_{1A} = Tier_{2A} = Tier_{2B} \neq Tier_{1B}, \tag{40}$$

$$Tier_{1A} = Tier_{1B} = Tier_{2B} \neq Tier_{2A}, \tag{41}$$

$$Tier_{1A} = Tier_{1B} = Tier_{2A} \neq Tier_{2B}. \tag{42}$$

Table 3. Isomorphic μ_p-γ-equivalent tiers. This table summarizes the variation in the tiers for the different approximation methods across the asset sets at the 95% confidence level ($\delta = 5\%$).

Variation of Tiers	Three-Year Estimation	Five-Year Estimation	Ratio
$Tier_{1A} = Tier_{1B} = Tier_{2A} = Tier_{2B}$	2011, 2012, 2013, 2014 2015, 2016, 2017, 2018 2019, 2020	2011, 2014, 2016, 2017 2018, 2020	80%
$Tier_{1A} = Tier_{1B} \neq Tier_{2A} = Tier_{2B}$		2015	5%
$Tier_{1A} = Tier_{2A} \neq Tier_{1B} = Tier_{2B}$		2013	5%
$Tier_{1B} = Tier_{2A} = Tier_{2B} \neq Tier_{1A}$		2012	5%
$Tier_{1A} = Tier_{2A} = Tier_{2B} \neq Tier_{1B}$			0%
$Tier_{1A} = Tier_{1B} = Tier_{2B} \neq Tier_{2A}$		2019	5%
$Tier_{1A} = Tier_{1B} = Tier_{2A} \neq Tier_{2B}$			0%

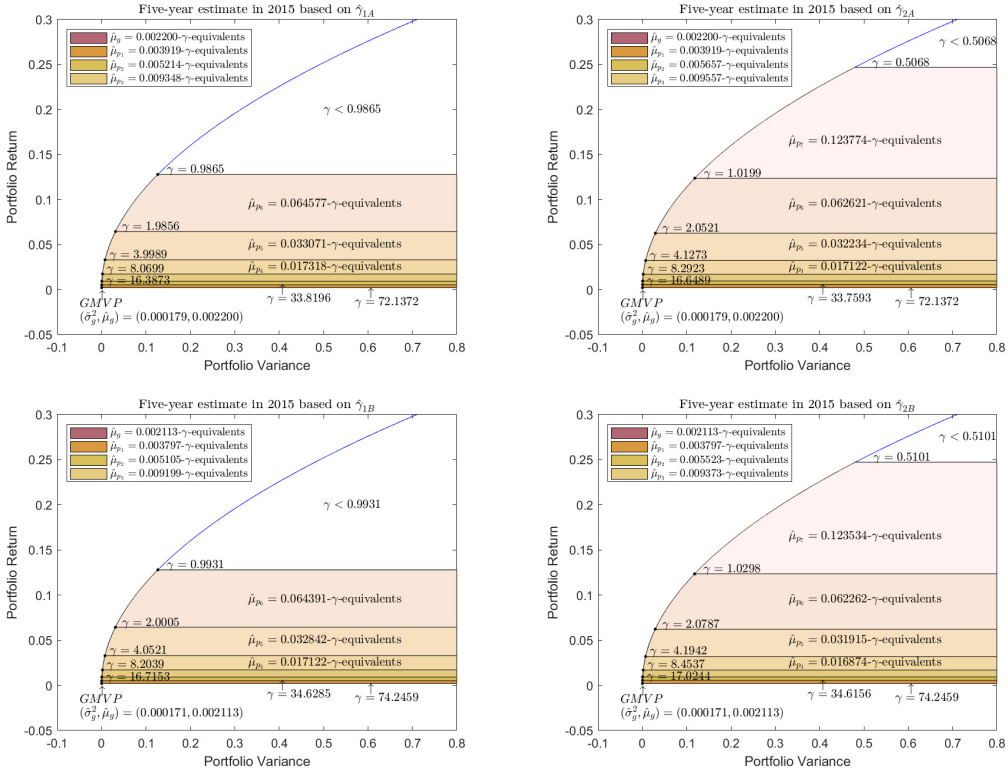


Figure 4. Tier variations due to approximation methods. This figure illustrates the approximation effect (37), where the tiers based on the first-degree approximations (**left panel**) differ from those based on the second-degree approximations (**right panel**).

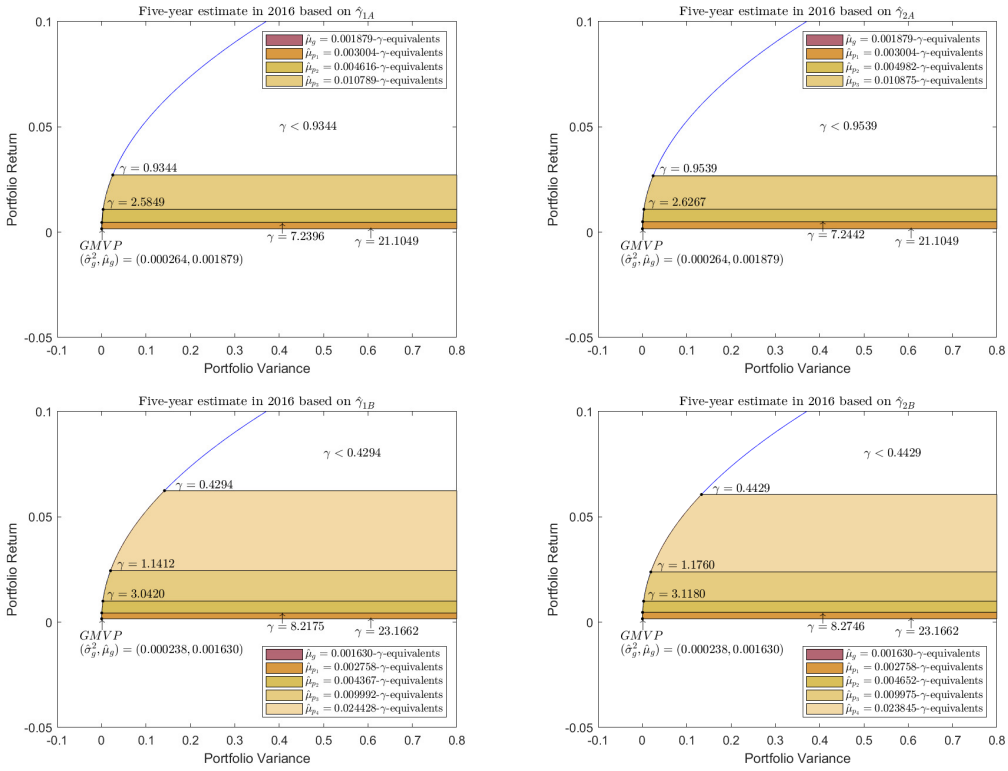


Figure 5. Tier variations due to assets sets. This figure illustrates the asset effect, where the tiers based on asset sets consisting exclusively of stocks (**top panel**) different from those based on the expanded asset sets including bonds (**bottom panel**).

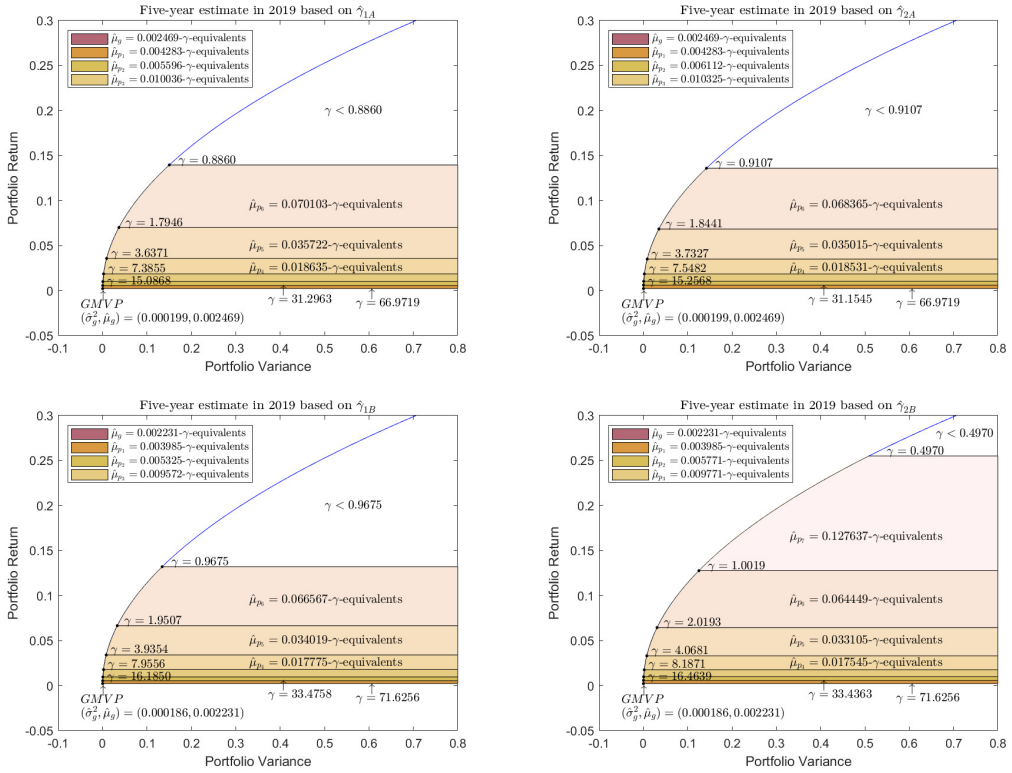


Figure 6. Tier variations due to mixed effects. This figure shows a mixed effect (42), where the bottom-right estimate $Tier_{2B}$ has a significantly different lower limit (L) among the four calculations. The (**top**) and (**bottom**) panels reveal the mixed effect caused by two different asset sets. Meanwhile, the (**left**) and (**right**) panels indicate the approximation effect. Likewise, the two cases (39)–(41) refer to the significant differences between the top-left estimate ($Tier_{1A}$), bottom-left estimate ($Tier_{1B}$), and top-right estimate ($Tier_{2A}$) in comparison to the other three equal estimates.

4.5. Results from Simulated Data

The example in Section 4.4 only exhibits seven tier variations. There may be other combinations, such as $Tier_{1A} = Tier_{1B} \neq Tier_{2B} \neq Tier_{2A}$. In this section, we simulate portfolios in order to analyze how the tiers depend on the portfolio size, the domain of γ, and other factors. From the complete set of assets, we randomly sampled assets to form a portfolio with size $N = 5$, 10, 15, and 20 stocks or 6, 11, 16, and 21 assets (the corresponding stocks plus bonds) in order to estimate γ_{1A}, γ_{1B}, γ_{2A}, and γ_{2B}. We repeated our simulation 2000 times, obtaining a total of 240,000 μ_p-γ equivalents (including the 10-year rolling window) at the 95% confidence level.

Additionally, we rounded up the average tier to the nearest integer for conservative estimations. Table 4 reports the classification of variation between the simulated tiers. The number of estimated tiers ranges from 3 to 8. The simulated results have no exceptions outside Equations (36)–(42). The simulated results are available from the corresponding author upon request.

To explore the potential factors of tier variations, we conducted multivariate regression based on the μ_p-γ equivalents:

$$Tiers_t = Con + a \times GM_t + b \times AM_t + c \times AS_t + d \times Size_t + e \times EW_t + u_t \quad (43)$$

where Equation (43) regresses the average tiers (and the roundup tiers) based on the following variables: GM (the domain of γ), AM (the first- and second-degree approximation methods), AS (the assets set with or without bonds), portfolio size, and EW (the estimation window).

Table 4. Classification of variations in the simulated tiers.

		Size of 3-Year Estimation				Size of 5-Year Estimation				
Year	**Equation**	**5**	**10**	**15**	**20**	**5**	**10**	**15**	**20**	**Ratio (%)**
2011	(36)	1367	1453	1419	1159	1623	1718	1718	1715	76.08
	(37)	0	0	0	0	0	2	8	3	0.08
	(38)	593	409	432	568	333	201	122	90	17.18
	(39)	11	53	50	136	9	36	61	94	2.81
	(40)	0	0	0	0	1	0	0	0	0.01
	(41)	1	0	0	0	5	0	0	0	0.04
	(42)	28	85	99	137	29	43	91	98	3.81
2012	(36)	1382	1606	1784	1870	1332	1427	1602	1759	79.76
	(37)	0	0	9	34	0	0	1	0	0.28
	(38)	599	326	104	40	610	401	272	97	15.31
	(39)	1	26	51	24	12	62	66	23	1.66
	(40)	0	0	2	8	0	0	0	0	0.06
	(41)	3	0	0	3	2	0	0	0	0.05
	(42)	15	42	50	21	44	110	59	121	2.89
2013	(36)	1831	1908	1907	1872	1349	1584	1587	1632	85.44
	(37)	0	1	9	22	0	0	0	0	0.20
	(38)	160	66	28	13	631	399	382	320	12.49
	(39)	0	4	7	11	0	7	18	19	0.41
	(40)	3	6	12	46	6	0	0	0	0.46
	(41)	6	8	17	34	14	0	0	0	0.49
	(42)	0	7	20	2	0	10	13	29	0.51
2014	(36)	1876	1917	1902	1867	1710	1889	1954	1965	94.25
	(37)	1	1	4	11	0	0	1	3	0.13
	(38)	97	49	36	32	270	104	29	5	3.89
	(39)	5	3	6	3	0	1	4	1	0.14
	(40)	8	10	24	37	2	1	2	8	0.58
	(41)	10	17	20	45	18	4	6	17	0.86
	(42)	3	3	8	5	0	1	4	1	0.16
2015	(36)	1842	1840	1822	1815	1723	1818	1832	1868	91.00
	(37)	4	7	23	44	0	2	3	10	0.58
	(38)	125	88	46	28	257	152	116	50	5.39
	(39)	4	20	20	28	3	9	28	38	0.94
	(40)	10	12	21	21	6	0	1	3	0.46
	(41)	10	7	26	35	10	2	2	13	0.66
	(42)	5	26	42	29	1	17	18	18	0.98
2016	(36)	1954	1902	1877	1756	1909	1942	1938	1938	95.10
	(37)	0	19	44	96	0	0	2	15	1.10
	(38)	25	15	3	3	63	43	12	9	1.08
	(39)	4	8	26	88	19	1	9	7	1.01
	(40)	8	22	10	0	3	7	12	3	0.41
	(41)	7	25	10	3	3	5	26	25	0.65
	(42)	2	9	30	54	3	2	1	3	0.65
2017	(36)	1911	1880	1848	1837	1897	1931	1913	1929	94.66
	(37)	0	2	27	44	1	0	0	0	0.46
	(38)	62	45	13	4	69	56	58	42	2.18
	(39)	3	1	1	0	17	5	0	0	0.17
	(40)	13	43	57	49	4	1	14	13	1.21
	(41)	8	28	49	65	7	4	15	16	1.20
	(42)	3	1	5	1	5	3	0	0	0.11
2018	(36)	1923	1911	1899	1847	1762	1878	1839	1829	93.05
	(37)	0	15	40	94	5	3	21	31	1.31
	(38)	62	18	4	2	221	82	40	14	2.77
	(39)	3	8	21	12	2	20	52	50	1.05
	(40)	5	18	6	10	2	1	2	0	0.28
	(41)	6	20	9	11	5	9	15	46	0.76
	(42)	1	10	21	24	3	7	31	30	0.79

Table 4. *Cont.*

Year	Equation	Size of 3-Year Estimation				Size of 5-Year Estimation				Ratio (%)
		5	10	15	20	5	10	15	20	
2019	(36)	917	1164	1190	1251	1309	1585	1591	1627	66.46
	(37)	0	0	0	0	0	0	0	0	0.00
	(38)	1044	791	726	638	670	383	333	283	30.43
	(39)	8	17	35	39	2	20	39	60	1.38
	(40)	0	0	0	0	1	0	0	0	0.01
	(41)	6	0	0	0	13	1	0	0	0.13
	(42)	25	28	49	72	5	11	37	30	1.61
2020	(36)	1582	1657	1642	1665	1903	1940	1913	1878	88.63
	(37)	0	0	0	0	1	2	8	19	0.19
	(38)	373	241	234	151	68	26	17	6	6.98
	(39)	16	44	56	76	13	19	33	57	1.96
	(40)	0	0	0	0	0	0	0	0	0.00
	(41)	2	0	0	0	13	6	5	18	0.28
	(42)	27	58	68	108	2	7	24	22	1.98

Table 5 reports the statistics based on Equation (43). Note that the results of the analysis for the average and roundup tiers are similar. For simplicity, we focus on the regression using only average tiers as the dependent variable. We make four observations from Table 5. First, the t-statistic of 13.3206 indicates a strongly positive relationship between the tiers and the γ domain estimation, with a larger γ domain yielding more tiers. Second, Table 5 fails to reject the null hypothesis of approximation and asset effects. However, the approximation and assets may revert their impact on the mixed effects through particular combinations, such as $Tier_{1A}$ and $Tier_{2B}$.

Table 5. Regression analysis of tiers' potential factors. This table summarizes the regression results (43) obtained when using the simulated results. Two types of regression tests were performed, based on the average tiers and roundup tiers. The notations **, and *** indicate that the statistic is significantly different from zero at the 5%, and 1% levels, respectively.

Variable	Average Tiers ($R^2 = 0.7147$)		Roundup Tiers ($R^2 = 0.6076$)		Observation
	Coefficient	t-Statistic	Coefficient	t-Statistic	
Constant	2.9490	30.4017 ***	3.6450	34.1056 ***	600
	(0.0970)		(0.1069)		
Domain of γ	0.0248	13.3206 ***	0.0262	12.7709 ***	600
	(0.0019)		(0.0020)		
Approximation	0.0358	0.6320	0.0266	0.4252	600
	(0.0567)		(0.0625)		
Assets set	−0.0136	−0.2398	0.0341	0.5441	600
	(0.0568)		(0.0626)		
Portfolio size	0.0777	15.9478 ***	0.0542	10.0936 ***	600
	(0.0049)		(0.0054)		
Window	−0.0259	−2.6237 ***	−0.0249	−2.2854 **	600
	(0.0099)		(0.0109)		

Third, Table 5 confirms the negative tier's horizon dependence. The t-statistic of −2.6237 indicates a strongly negative relation between the number of tiers and the estimation window, with a longer estimation window yielding fewer tiers. Our results are consistent with those of Bliss and Panigirtzoglou [6], who concluded that the intensely estimated γ horizon dependence results from short-horizon investors are more risk-averse and less flexible.

Finally, Table 5 shows that all rows reveal a positive correlation between the average tiers of μ_p-γ-equivalent and the portfolio size for each year and each estimation window.

The size highlights this strong positive correlation between the tiers and portfolio size at the 1% level, with a significant t-statistic of 15.9478.

5. Conclusions

Investors often use a risk aversion attitude to regulate their investment decisions, with the capital asset pricing model (CAPM) developed by Sharpe [35], Lintner [36], and Mossin [37] being the most popular model for this purpose. For simplicity, investors and researchers typically assign a number from 1 to M to their risk aversion coefficients. After employing risk aversion, investors need to estimate the parameters of the efficiency frontier such that some adjacent portfolios show statistically insignificant isomorphic risk aversion coefficients. Non-institutional investors in particular tend to make decisions based on their risk aversion coefficients. This common practice of determining the risk aversion coefficient can become even more ambiguous when considering the uncertainty of various parameters.

To address the ambiguity of risk aversion, in this paper we develop first- and second-degree approximations of the risk aversion coefficients. Based on the relationship between the risk aversion coefficient and the efficient set of constants, we construct the approximate confidence interval for the risk aversion coefficient given a target return from both the return and variance perspectives. Our approach generalizes Bodnar and Okhrin's GMVP-equivalents to non-GMVP-equivalents and segments the mean-variance portfolios according to a hierarchy of risk aversion coefficients. We show that the hierarchical risk aversion coefficients outperform isometric attributes. Additionally, evidence is provided indicating that the portfolio size is the determining factor for the number of tiers.

In this study, we have estimated the risk aversion coefficient of the inductive isomorphic portfolio, which can assist investors in simplifying numerous portfolios into hierarchical risk aversion coefficients. Our findings will aid investors (particularly non-institutional investors) in their decision-making while also streamlining their process, thereby relieving them of the complexity of dealing with many portfolios. For example, investors can use the expected utility preference framework to allocate a limited budget. Therefore, non-professional investors may purchase exchange-traded funds (ETFs) or use fractional trading to offset risk-averse behaviors. While this trading model allows non-institutional investors to be more active in increasing their participation in the market, it must be exposed to the risk of high volatility. Therefore, the tiered investment group classification obtained in this study allows non-institutional investors to choose a homogeneous portfolio that is not at the highest level of risk.

The approximations presented in this study have limitations in application, mainly when considering two portfolios with isomorphic risk aversion coefficients, as these may overlap in such a way that they cannot be accurately divided. In addition, the inclusion of new financial products (e.g., digital assets) must be taken into consideration during optimization due to the limited sample size. Therefore, future extensions to this work could involve extending the hierarchical risk aversion framework to other approximations that allow for more accurate portfolio segmentation and introducing digital assets with option-like features.

Funding: National Science and Technology Council of Taiwan grant number MOST 111-2410-H-239-008 funded this research, and the APC was funded by the National Science and Technology Council of Taiwan, grant number NSTC 113-2410-H-239-015.

Data Availability Statement: Data is unavailable due to ethical restrictions.

Acknowledgments: The author is grateful to the anonymous Reviewers for their helpful suggestions which improved the presentation of the paper.

Conflicts of Interest: The authors declare no conflicts of interest.

Appendix A. Proof of Theorem 2

Conditional on $\hat{\psi}$ in Lemma 2, we straightforwardly derive a series of the product moments of the sample efficient set constants:

$$
\begin{aligned}
E(\hat{\psi}\hat{\mu}_g) &= E(E(\hat{\psi}\hat{\mu}_g|\hat{\psi})) = E(\hat{\psi}E(\hat{\mu}_g|\hat{\psi})) = E(\hat{\psi})\mu_g = \left[\tfrac{N-1+T\psi}{(T-N-1)}\right]\mu_g,\\
E(\hat{\psi}\hat{\mu}_g^2) &= E(\hat{\psi})\left(\mu_g^2 + \tfrac{\sigma_g^2(T-N)}{T^2}\right) + E(\hat{\psi}^2)\left(\tfrac{\sigma_g^2(T-N)}{T^2}\right),\\
E(\hat{\psi}\hat{\mu}_g^3) &= E(\hat{\psi})\left(\mu_g^3 + \tfrac{3\sigma_g^2(T-N)\mu_g}{T^2}\right) + E(\hat{\psi}^2)\left(\tfrac{3\sigma_g^2(T-N)\mu_g}{T^2}\right),\\
E(\hat{\psi}\hat{\mu}_g^4) &= E(\hat{\psi})\left(\mu_g^4 + \tfrac{6\sigma_g^2(T-N)\mu_g^2}{T^2} + \tfrac{3\sigma_g^4(T-N)(T-N+2)}{T^4}\right),\\
&\quad + E(\hat{\psi}^2)\left(\tfrac{6\sigma_g^2(T-N)\mu_g^2}{T^2} + \tfrac{6\sigma_g^4(T-N)(T-N+2)}{T^4}\right) + E(\hat{\psi}^3)\left(\tfrac{3\sigma_g^4(T-N)(T-N+2)}{T^4}\right),\\
E(\hat{\psi}^2\hat{\mu}_g^2) &= E(\hat{\psi}^2)\left(\mu_g^2 + \tfrac{\sigma_g^2(T-N)\mu_g}{T^2}\right) + E(\hat{\psi}^3)\left(\tfrac{\sigma_g^2(T-N)\mu_g}{T^2}\right),\\
E(\hat{\psi}^2\hat{\mu}_g^3) &= E(\hat{\psi}^2)\left(\mu_g^3 + \tfrac{3\sigma_g^2(T-N)\mu_g}{T^2}\right) + E(\hat{\psi}^3)\left(\tfrac{3\sigma_g^2(T-N)\mu_g}{T^2}\right),\\
E(\hat{\psi}^2\hat{\mu}_g^4) &= E(\hat{\psi}^2)\left(\mu_g^4 + \tfrac{6\sigma_g^2(T-N)\mu_g^2}{T^2} + \tfrac{3\sigma_g^4(T-N)(T-N+2)}{T^4}\right)\\
&\quad + E(\hat{\psi}^3)\left(\tfrac{6\sigma_g^2(T-N)\mu_g^2}{T^2} + \tfrac{6\sigma_g^4(T-N)(T-N+2)}{T^4}\right) + E(\hat{\psi}^4)\left(\tfrac{3\sigma_g^4(T-N)(T-N+2)}{T^4}\right).
\end{aligned}
$$

Second, based on those moments of $E(\hat{\psi}\hat{\mu}_g^h)$, $h = 1, 2, 3, 4$ and $E(\hat{\psi}^2\hat{\mu}_g^k)$, $k = 2, 3, 4$, the expected value and the variance of $\hat{\gamma}_1$ are computed as

$$
\begin{aligned}
E(\hat{\gamma}_1) &= \tfrac{1}{\mu_p}\left(E(\hat{\psi}) + \tfrac{E(\hat{\psi}\hat{\mu}_g)}{\mu_p}\right) = \tfrac{1}{\mu_p}\left[\tfrac{N-1+T\psi}{(T-N-1)} + \tfrac{\mu_g}{\mu_p} \times \tfrac{N-1+T\psi}{(T-N-1)}\right],\\
V(\hat{\gamma}_1) &= \tfrac{1}{\mu_p^2}\left(V(\hat{\psi}) + \tfrac{2Cov(\hat{\psi},\hat{\psi}\hat{\mu}_g)}{\mu_p} + \tfrac{V(\hat{\psi}\hat{\mu}_g)}{\mu_p^2}\right) = \tfrac{V(\hat{\psi})T^2(\mu_p+\mu_g)^2 + E(\hat{\psi}^2)(T-N)\sigma_g^2 + E(\hat{\psi}^3)(T-N)\sigma_g^2}{T^2\mu_p^4}.
\end{aligned}
$$

where

$$
\begin{aligned}
Cov(\hat{\psi}, \hat{\psi}\hat{\mu}_g) &= E(E(\hat{\psi}^2\hat{\mu}_g|\hat{\psi})) - E(\hat{\psi})E(\hat{\psi}\hat{\mu}_g) = V(\hat{\psi})\mu_g,\\
V(\hat{\psi}\hat{\mu}_g) &= E(E(\hat{\psi}^2\hat{\mu}_g^2|\hat{\psi})) - (E(\hat{\psi}\hat{\mu}_g))^2 = \tfrac{E(\hat{\psi}^2)(T-N)\sigma_g^2}{T^2} + \tfrac{E(\hat{\psi}^3)(T-N)\sigma_g^2}{T^2} + V(\hat{\psi})\mu_g^2,
\end{aligned}
$$

Lastly, Equation (25) provides the expected value and the variance of $\hat{\gamma}_2$ in a similar manner:

$$
\begin{aligned}
E(\hat{\gamma}_2) &= E(\hat{\gamma}_1) + \tfrac{E(\hat{\psi}\hat{\mu}_g^2)}{\mu_p^3} = E(\hat{\psi})\left(\tfrac{1}{\mu_p} + \tfrac{\mu_g}{\mu_p^2} + \tfrac{\mu_g^2}{\mu_p^3} + \tfrac{\sigma_g^2(T-N)}{T^2\mu_p^3}\right) + E(\hat{\psi}^2)\left(\tfrac{\sigma_g^2(T-N)}{T^2\mu_p^3}\right),\\
V(\hat{\gamma}_2) &= V(\hat{\gamma}_1) + 2Cov(\hat{\gamma}_1, \hat{\gamma}_e) + V(\hat{\gamma}_e),\\
V(\hat{\gamma}_e) &= \tfrac{V(\hat{\psi}\hat{\mu}_g^2)}{\mu_p^6} = \tfrac{E(\hat{\psi}^2\hat{\mu}_g^4) - \left(E(\hat{\psi}\hat{\mu}_g^2)\right)^2}{\mu_p^6},\\
Cov(\hat{\gamma}_1, \hat{\gamma}_e) &= \tfrac{E(\hat{\psi}^2\hat{\mu}_g^2)}{\mu_p^4} + \tfrac{E(\hat{\psi}^2\hat{\mu}_g^3)}{\mu_p^5} - \left(\tfrac{E(\hat{\psi})}{\mu_p} + \tfrac{E(\hat{\psi}\hat{\mu}_g)}{\mu_p^2}\right)\left(\tfrac{E(\hat{\psi}\hat{\mu}_g^2)}{\mu_p^3}\right).
\end{aligned}
$$

References

1. Markowitz, H. Portfolio selection. *J. Financ.* **1952**, *7*, 77–91.
2. Stevens, G.V.G. On the inverse of the covariance matrix in portfolio analysis. *J. Financ.* **1998**, *53*, 1821–1827. [CrossRef]
3. Kan, R.; Zhou, G. Optimal portfolio choice with parameter uncertainty. *J. Financ. Quant.* **2007**, *42*, 621–656. [CrossRef]
4. Jackwerth, J.C. Recovering risk aversion from option prices and realized returns. *Rev. Financ. Stud.* **2000**, *13*, 433–451. [CrossRef]
5. Guisoa, L.; Sapienza, P.; Zingales, L. Time varying risk aversion. *J. Financ. Econ.* **2018**, *128*, 403–421. [CrossRef]
6. Bliss, R.R.; Panigirtzoglou, N. Option-implied risk-aversion estimates. *J. Financ.* **2004**, *68*, 407–446. [CrossRef]
7. Stambaugh, R.F. Analyzing investments whose histories differ in length. *J. Financ. Econ.* **1997**, *45*, 285–331. [CrossRef]
8. Brandt, M.W.; Santa-Clara, P. Dynamic portfolio selection by augmenting the asset space. *J. Financ.* **2006**, *61*, 2187–2217. [CrossRef]
9. DeMiguel, V.; Garlappi, L.; Uppal, R. Optimal versus naive diversification: How inefficient is the 1/N portfolio strategy? *Rev. Financ. Stud.* **2009**, *22*, 1915–1953. [CrossRef]

10. Aït-Sahalia, Y.; Lo, A.W. Nonparametric risk management and implied risk aversion. *J. Econom.* **2000**, *94*, 9–51. [CrossRef]
11. Bodnar, T.; Okhrin, Y. Boundaries of the risk aversion coefficient: Should we invest in the global minimum variance portfolio? *Appl. Math. Comput.* **2013**, *219*, 5440–5448. [CrossRef]
12. Das, S.; Markowitz, H.; Scheid, J.; Statman, M. Portfolio optimization with mental accounts. *J. Financ. Quant. Anal.* **2010**, *45*, 311–334. [CrossRef]
13. Das, S.; Markowitz, H.; Scheid, J.; Statman, M. Portfolios for investors who want to reach their goals while staying on the mean-variance efficient frontier. *J. Wealth Manag.* **2011**, *14*, 25–31. [CrossRef]
14. De Nardi, M.; French, E.; Jones, J.B. Why do the elderly save? The role of medical expenses. *J. Political Econ.* **2010**, *118*, 39–75. [CrossRef]
15. De Nardi, M.; Yang, F. Bequests and heterogeneity in retirement wealth. *Eur. Econ. Rev.* **2014**, *72*, 182–196. [CrossRef]
16. Dickinson, J.P. The reliability of estimation procedures in portfolio analysis. *J. Financ. Quant.* **1974**, *9*, 447–462. [CrossRef]
17. Klein, R.; Bawa, V. The effect of estimation risk on optimal portfolio choice. *J. Financ. Econ.* **1976**, *3*, 215–231. [CrossRef]
18. Jobson, J.D.; Korkie, B. Estimation for Markowitz efficient portfolios. *J. Am. Stat. Assoc.* **1980**, *75*, 544–554. [CrossRef]
19. Best, M.J.; Grauer, R.R. On the sensitivity of mean-variance portfolios to change in asset means: Some analytical and computation results, and the structure of asset expected returns. *Rev. Financ. Stud.* **1991**, *4*, 315–342. [CrossRef]
20. Jobson, J.D. Confidence regions for the mean-variance efficient set: An alternative approach to estimation risk. *Rev. Quant. Financ. Account.* **1991**, *1*, 235–257. [CrossRef]
21. Britten-Jones, M. The sampling error in estimating of mean-variance efficient portfolio weights. *J. Financ.* **1999**, *54*, 655–671. [CrossRef]
22. Okhrin, Y.; Schmid, W. Distributional properties of portfolio weights. *J. Econom.* **2006**, *134*, 235–256. [CrossRef]
23. Kan, R.; Smith, D.R. The distribution of the sample minimum-variance frontier. *Manag. Sci.* **2008**, *54*, 1364–1380. [CrossRef]
24. Chiu, W.Y. Mean-variance hedging in the presence of estimation risk. *Rev. Deriv. Res.* **2021**, *24*, 221–241. [CrossRef]
25. Merton, R.C. An analytic derivation of the efficient portfolio frontier. *J. Financ. Quant. Anal.* **1972**, *7*, 1851–1872. [CrossRef]
26. Roll, R. A critique of the asset pricing theory's tests. *J. Financ. Econ.* **1977**, *4*, 129–176. [CrossRef]
27. Kroll, Y.; Levy, H.; Markowitz, H. Mean-variance versus direct utility maximization. *J. Financ.* **1984**, *39*, 47–61.
28. Ingersoll, J.E. *Theory of Financial Decision Making*; Rowman Littlefield Publishers: Lanham, MD, USA, 1987.
29. Bodnar, T.; Parolya, N.; Schmid, W. On the equivalence of quadratic optimization problems commonly used in portfolio theory. *Eur. J. Oper. Res.* **2013**, *229*, 637–644. [CrossRef]
30. Bodnar, T.; Schmid, W. Estimation of optimal portfolio compositions for Gaussian returns. *Stat. Decis.* **2008**, *26*, 179–201. [CrossRef]
31. Bodnar, T.; Schmid, W. Econometric analysis of the sample efficient frontier. *Eur. J. Financ.* **2009**, *15*, 317–335. [CrossRef]
32. Muirhead, R. *Aspects of Multivariate Statistical Analysis*; Wiley: New York, NY, USA, 1982.
33. Patnaik, P.B. The Non-central χ^2- and F-distributions and their applications. *Biometrika* **1949**, *36*, 202–232. [CrossRef] [PubMed]
34. Tang, G.Y.N. How efficient is naive portfolio diversification? An educational note. *Omega* **2004**, *32*, 155–160. [CrossRef]
35. Sharpe, W.F. Capital asset prices: A theory of market equilibrium under conditions of risk. *J. Financ.* **1964**, *19*, 425–442.
36. Lintner, J. The valuation of risk assets and the slection of risky investment in stock and capital budgets. *Rev. Econ. Stat.* **1964**, *47*, 13–37. [CrossRef]
37. Mossin, J. Equilibrium in a Capital Asset Market. *Econometrica* **1966**, *34*, 768–783. [CrossRef]

Disclaimer/Publisher's Note: The statements, opinions and data contained in all publications are solely those of the individual author(s) and contributor(s) and not of MDPI and/or the editor(s). MDPI and/or the editor(s) disclaim responsibility for any injury to people or property resulting from any ideas, methods, instructions or products referred to in the content.